NINETY-TWO YEARS OF TREE GROWTH AND DEATH IN A SECOND-GROWTH COAST REDWOOD FOREST

By

Benjamin G. Iberle

A Thesis Presented to

The Faculty of Humboldt State University

In Partial Fulfillment of the Requirements for the Degree

Master of Science in Natural Resources: Forest, Watershed, and Wildland Sciences

Committee Membership

Dr. Stephen C. Sillett, Committee Chair

Dr. Robert Van Pelt, Committee Member

Dr. Jeffrey M. Kane, Committee Member

Dr. Alison P. O'Dowd, Graduate Coordinator

December 2016

ABSTRACT

NINETY-TWO YEARS OF TREE GROWTH AND DEATH IN A SECOND-GROWTH COAST REDWOOD FOREST

Benjamin G. Iberle

Mature second-growth coast redwood (*Sequoia sempervirens*) forests are an important and uncommon resource in the redwood region. Development of second-growth redwood forests beyond rotation age (~50 years) is not well understood. Continuous long-term data are especially lacking, considering that the maximum possible age of second-growth stands is now over 150 years. Two permanent observation plots in Arcata, CA, established in 1923 by Woodbridge Metcalf and last measured in 1990, provide a unique opportunity to examine the development of coast redwood forest regenerating after logging in ~1880. We surveyed the Metcalf plots using modern methods and assembled a complete dataset from 1923 to 2015. We also built new allometric models for second-growth coast redwood to predict tree-level quantities such as total biomass and leaf area from ground-based measurements. The Metcalf plots nearly doubled in total basal area over the study period, reaching 124 and 143 m^2 ha^{-1}, and redwood increased in proportional dominance as the non-redwood species steadily declined in number. These results, along with substantial density-independent mortality, suggest a transition to a maturation stage of forest development at ~83 years since logging. In the most recent surveys (~135 years since logging), the leaf area index values

of trees alone for the Metcalf plots (9.8 and 12.7) are similar to nearby old-growth forests (11.6-15.9). Our results from relatively unmanaged conditions can be compared to silvicultural treatments of regenerating coast redwood forest meant to accelerate development of old-growth characteristics, especially as treated stands move beyond rotation age.

ACKNOWLEDGMENTS

Thank you to Allyson Carroll, Ethan Coonen, Bill Kruse, and the Fall 2013 Forest Measurements class at HSU for their assistance with data collection and preparation. This project would not have been possible without the cooperation of the City of Arcata and collaboration with Mark Andre. Support was provided by the Kenneth L. Fisher Chair of Redwood Forest Ecology at Humboldt State University and the Save the Redwoods League.

TABLE OF CONTENTS

LIST OF TABLES

LIST OF FIGURES

INTRODUCTION

Sequoia sempervirens (hereafter *Sequoia*) is the tallest species (Sillett et al., 2015) and has the global maximum capacity for accumulating forest biomass (Van Pelt et al., 2016). Beyond its superlative nature, *Sequoia* (or coast redwood) is the dominant tree species in a unique forested ecosystem occupying much of the northwestern California coast (Noss, 2000). However, over 95% of these forests have been logged since the arrival of European settlers, and most of those forests have been logged at least once more since then (Sawyer et al., 2000). Mature second-growth forests, which have only been logged once, are an important and uncommon resource in the redwood region. Second-growth *Sequoia* forests are a source of much-needed habitat for threatened species, carbon sequestration, and economic and social value (Thornburgh et al., 2000). Unfortunately, development of second-growth *Sequoia* forests beyond rotation age is not well understood. Continuous long-term data are especially lacking, considering that the maximum possible age of second-growth stands is now over 150 years. Additionally, *Sequoia* forests may require more than 500 years to reach an old-growth state (Van Pelt et al., 2016), highlighting that much of the developmental sequence has yet to be observed.

Although the rate of change throughout the complete trajectory is unknown, differences between young- and old-growth *Sequoia* forests are easily identified. All *Sequoia* forests, which are dominated by a species that is shade tolerant, sprouts prolifically from lignotubers (Del Tredici, 1998; Neal, 1967), and can live for over 2500

years (Sillett et al., 2015), occur along the California coast from Big Sur to extreme southwestern Oregon. Depending on a forest's location within the range, as well as site quality and history, *Sequoia* shares the canopy with other tree species, such as *Pseudotsuga menziesii*, *Abies grandis*, *Picea sitchensis*, *Tsuga heterophylla*, *Thuja plicata*, *Notholithofagus densiflorus*, *Umbellularia californica*, and *Acer macrophyllum* (Sawyer et al., 2000). Stand-replacing wildfires are extremely rare (Lorimer et al., 2009), so old-growth *Sequoia* forests typically have multi-layered canopies and a broad tree age distribution (Sawyer et al., 2000). These forests experience slow rates of individual tree turnover with large canopy gaps opened infrequently (Busing and Fujimori, 2002), resulting in high diversity in horizontal structure. Emergent trees with deep crowns facilitate global maximum leaf area index by increasing understory light availability (Van Pelt et al., 2016). In comparison, regenerating *Sequoia* forests are structurally simple and relatively uniform. After the stand-replacing disturbance of logging, the regenerating forests typically progress through a stand development sequence (Franklin et al., 2002). Non-*Sequoia* tree species may be more prevalent, depending on local conditions (e.g., advance regeneration, legacy trees, aerial seeding, prescribed burns). Shade-tolerant and fire-adapted *Sequoia* will eventually dominate the canopy, but this process may be delayed by fire exclusion and other human disturbances and management practices (Thornburgh et al., 2000).

The scientific literature on mature second-growth *Sequoia* forest (logged > 100 years ago) is sparse. The longest existing dataset is from a single one-acre permanent plot on a river terrace in Big River, CA (Mendocino County) which exhibited very high rates

of tree growth since establishment in 1923 (Allen et al., 1996; Fritz, 1945; Gerhart, 2006). This rich alluvial forest plot was nicknamed the "Wonder Plot" due to its phenomenal growth rate. A chronosequence analysis showed that second growth can approach old growth in stem density and canopy cover within 130 years (Russell and Michels, 2011), but there are still large differences in basal area, *Sequoia* dominance, and tree structure (Van Pelt et al., 2016). Accelerating the development of such characteristics in regenerating forests with silvicultural techniques is an expanding area of research, and most studies only span a short period (15-25 years) after treatment. Experiments confirm that thinning can increase *Sequoia* growth and dominance (Chittick et al., 2007; Lindquist, 2004; Plummer et al., 2012; Teraoka, 2012; Webb et al., 2012).

Permanent observation plots established in 1923 in Arcata, California provide a unique opportunity to examine the development of second-growth *Sequoia* forest. Woodbridge Metcalf (University of California, Berkeley) established two one-acre plots (hereafter called the "Metcalf plots") in forest largely unmanaged since being logged around 1880 and seven surveys were completed between 1923 and 1990. The Metcalf plots can expand the temporal, as well as geographical, range of data on *Sequoia* forests. Previous research on mature second-growth (Gerhart, 2006; Russell and Michels, 2011) occurred in the central range of *Sequoia*, characterized by pure stands on alluvial flats with little undergrowth and upland stands that have a mixture of *P. menziesii* and *N. densiflorus* and understory shrubs (Sawyer et al., 2000). The Metcalf plots serve as a contrasting example of the wetter northern *Sequoia* forest type that sees the appearance of *P. sitchensis* and a denser understory dominated by *Polystichum munitum* (Sawyer et al.,

2000). Despite the small area sampled, this long-term dataset on relatively undisturbed forest presents an opportunity to build on our limited knowledge of *Sequoia* forest development into mature stages following logging.

In this study, we re-survey the Metcalf plots, extending the observed timespan to 92 years (i.e., 43–135 years since logging). Use of similar modern survey methods allowed us to compare current forest conditions to those described recently for old-growth *Sequoia* forests (Van Pelt et al., 2016). We also developed allometric equations to predict whole-tree quantities (e.g. total biomass, leaf area, wood volume) from ground-based measurements for *Sequoia* in regenerating forests using the same methods employed in recent studies (Coonen and Sillett, 2015; Sillett et al., 2015). New equations were needed for regenerating forests due to profound differences in light environment experienced by trees of similar stature in old-growth forests. Dendrochronological reconstructions of individual tree growth allowed us to check the accuracy of the allometric equations as well as the historical survey measurements.

Our objectives in this study are to: (1) assemble a complete dataset for the Metcalf plots spanning 1923 to present-day and examine trends in tree species composition, demographics, and growth, (2) compare results from the first objective to other long-term studies of second-growth *Sequoia* forests and to old-growth forest characteristics, and (3) compare tree growth estimates derived from ground-based measurements combined with allometric equations to those derived from dendrochronology combined with tree climbing measurements. Results from our study will provide insight into the structural

and compositional changes in mature second-growth forests that can inform management aimed at promoting old-growth forests characteristics.

METHODS

Allometric Models

Sequoia

New allometric equations for predicting whole-tree quantities (e.g. total mass, wood volume, leaf area) of *Sequoia* in regenerating forests utilized 32 trees from previous studies (12 trees from Sillett et al., 2015; 20 trees from Coonen and Sillett, 2015) and one tree from each plot. Trees ranged in size from 22.9 to 82.2 m tall and 34 to 209 cm functional DBH (i.e., diameter of a circle equal in area to trunk cross-section at 1.37 m, hereafter *f*DBH). Quantities for these trees were obtained non-destructively using intensive tree climbing measurements combined with branch-level allometrics (Coonen and Sillett, 2015; Sillett et al., 2015). The set of potential predictors of whole-tree quantities was *f*DBH, diameter at top of buttress (i.e., where trunk becomes mostly round, hereafter DTB), height, and crown volume. We built stepwise power functions for each dependent variable using the full set of predictors and selected models using AIC_c. We also built models to predict all dependent variables with *f*DBH alone, as many trees in the historical dataset were not measured for height, and none were measured for DTB or crown volume.

Non-*Sequoia*

Allometric equations for *Picea* and *Pseudotsuga* in coastal forests were developed with the same methods (S.C. Sillett, unpublished). For *Abies*, we used equations published in Standish et al. (1985) to predict total biomass, trunk volume, and leaf mass based on DBH and height. Most trees were only measured for height in a few surveys out of eight possible, so we predicted height to use the Standish equations. We built a power function predicting height from DBH using all *Abies* measured for height in the plots. This height curve was applied to each tree with zero or one height measurement and single height values were used to adjust the curve up or down. For trees with multiple height measurements, heights in intervening surveys were interpolated with a cubic spline.

Growth Reconstructions

We intensively measured two *Picea* and two *Sequoia* trees by accessing crowns with arborist-style climbing techniques. The trees selected were the tallest viable candidates for climbing that had definite matches and at least two height measurements in the historical surveys. All appendages were measured and mapped using protocols described previously (Coonen and Sillett, 2015; Sillett et al., 2015), providing data for the allometric models previously described. We also collected cores with increment borers from the main trunk at 10-15 m intervals. At each coring height, we measured trunk diameter, removed two cores, and measured bark thickness by inserting the probe of the borer back into the hole, locating the cambium, and using the probe to measure distance

from the cambium to the circumferential tape. Cores were mounted on wood blocks, sanded with progressively finer sandpaper (up to 1500 grit), and scanned at high resolution to permit annual ring widths to be measured to the nearest 0.001 mm using WinDENDRO (v. 2009) image analysis (Regent Instruments, Quebec, Canada). Cores were examined under a microscope to identify tight or wedged rings. We visually cross-dated each ring series at an annual resolution using the list method (Yamaguchi, 1991). Master chronologies and marker years used were from plots in Prairie Creek Redwoods State Park and Redwood National Park (Carroll et al., 2014). We verified our cross-dating with overlapping correlations calculated with the COFECHA program (Holmes, 1983).

Height, *f*DBH, and trunk volume of each tree was reconstructed using the cross-dated ring series. Calendar year of the pith anchored the height growth curve at each coring height. We interpolated between coring heights by scaling annual height growth based on annual radial growth (averaged between the two cores) from the uppermost ring series. For *f*DBH, we subtracted the average ring width for the breast height pair of cores from the previous year's wood radius for each successive year in the ring series, thus obtaining a history of wood radius. Bark radius was predicted based on each annual wood radius, using a power function built with the same dataset used for the whole-tree allometrics. Adding predicted bark radius to reconstructed wood radius produced the *f*DBH growth history. For main trunk wood growth, we reconstructed wood radius at every trunk diameter measurement height as we did at breast height. At measurement heights between cores, we used ring widths interpolated from the nearest overlying and

underlying cores. At measurement heights above the highest core, ring widths were assumed to be equal to those of the highest core. At measurement heights below the lowest core, we calculated ring widths by averaging ring widths of the lowest cores and ring widths of the lowest cores scaled up in proportion to the difference between diameter at core height and measurement height. Each year's reconstructed total height and all wood radii were used to calculate total trunk wood volume with conic frusta. We also predicted total trunk wood volume for each year by applying allometric equations to the reconstructed *f*DBH and height values.

Plot Surveys

Metcalf and associates established two square one-acre (0.4-ha) plots and thinned half of each in 1923. Plot 1 was thinned from below, primarily *Sequoia*, and Plot 2 was thinned from above, all non-*Sequoia*. About 18% of the standing basal area was removed in both treated plot halves. All trees were measured every ten years from 1923 to 1963, as well as in 1929. They recorded species, diameter at breast height (DBH), crown class, and painted an ID number on each tree (tags may have also been placed in 1963). Height was measured on a haphazard subset of trees in each survey with an unknown method. Minimum tree DBH was likely 7.6 cm (3 in), as only one tree smaller than that was recorded.

The plots were next surveyed in 1990 by Rudolf Becking (Humboldt State University) and associates. They collected the same data as the Metcalf surveys, although minimum tree DBH appears to have been 6 cm. The Metcalf tree IDs were recorded

when the paint was readable or a tag was present, and new IDs were assigned to trees with neither. They also mapped stem locations with visually approximated sketches.

The current surveys for Plot 1 and Plot 2 were completed in 2013 and 2015, respectively. All trees ≥ 5 cm in DBH (live and standing dead) were tagged at either breast height or top of buttress, whichever was higher. We determined ground level as the average of the lowest and highest points of ground around the tree base and measured DBH to the nearest 0.1 cm at exactly 1.37 m above that point. For trunks with buttressing, fused stems, or deformities, we used cross-sectional area at BH to calculate *f*DBH. Cross-sectional area was captured by sketching the cross-section with the assistance of tapes wrapped at BH and TB and then using ImageJ (National Institutes of Health, Bethesda, Maryland) to measure the area with tape wraps used for scale. We also measured height to crown base and crown radii in four cardinal directions. Crown volume was calculated using crown depth (total height minus height to crown base) and average crown radius as the dimensions of a paraboloid for *Sequoia* < 100 cm *f*DBH and all non-*Sequoia*. We used a smooth transition between paraboloid and prolate spheroid for *Sequoia* > 100 cm *f*DBH (Sillett et al., 2015). Species, snapped or dead tops, and other anomalies were also recorded. Finally, top diameter was measured directly or estimated on all stumps, snags, and broken trunks of live trees.

Challenges inherent in accurately measuring tree heights in tall forests necessitated use of three different methods, listed from first to last choice if more than one was available: laser rangefinder shot from the crown of one of the climbed trees, aerial LiDAR point cloud, and laser rangefinder shot from the ground. The aerial LiDAR

dataset provided a digital elevation model (DEM; ground-corrected in the plot, described below) and a canopy surface model (CSM). The DEM is prone to error at the scale needed for individual trees due to the canopy intercepting the majority of laser pulses, so we surveyed from the ground to improve the DEM. We measured elevation differences between landmarks with a laser rangefinder and subtracted them from the elevation differences calculated from the DEM. The residual error between ground survey and DEM was interpolated over the entire plot with Delaunay triangulation in QGIS (QGIS Development Team, 2012) and then added to the DEM to produce a corrected version. Peaks in the CSM were located as treetops and could be linked to trees with our geo-located stem map. Tree base elevations from the corrected DEM were subtracted from the CSM elevations to obtain tree heights. Heights measured with laser rangefinder from a known height while in the crown of a tree were converted to target tree height by accounting for the base elevations of the climbed tree and the target tree. All height measurements were made to the nearest 10 cm.

Exact plot corners were not initially known, so we surveyed all trees that might be within the plots based on the approximate 1990 maps. We then created an accurate stem map that could be used with LiDAR data and notes from plot establishment to place plot corners accurately for a square acre (63.6 × 63.6 m). Stem locations were mapped using a laser rangefinder and compass to measure distance and azimuth to either a fixed central point in a plot quadrant (Plot 1) or one of two fiberglass tapes stretched as transects across the plot (Plot 2). The plot quadrants/transects overlapped with each other so that shared trees could be used to create a single plot coordinate system. We checked stem

locations in the field against each other and available features (streams, trails, logs, etc.). The floating coordinate system for each plot was geo-located by lining up crown profiles from the LiDAR point cloud with those from our stem locations and field-measured crown radii. Plot corners were placed to include all known "in" trees and minimize differences with notes from 1923 on distances between known landmarks (e.g. distinctive trees) and plot boundaries.

Data Processing and Analysis

The original field datasheets from all previous surveys were transcribed and checked for missing data, errors, and inconsistencies. Single-year DBH measurements that were missed or clearly wrong were predicted with a cubic spline fitted to the individual tree's remaining DBH values with survey year as the predictor. We linked current trees and unlinked 1990 trees to original ID numbers using the 1990 stem maps, remaining tags, still legible painted numbers, and inference based on species, size, and identification number (assigned sequentially as they moved across the plot in 1923). We then checked again for errors and inconsistencies in the complete dataset.

Whole-tree values for all live tree observations were predicted using the previously described sets of allometric equations. Small (< 2 cm) decreases in DBH were observed in some slow-growing individuals, likely due to bark sloughing. Since bark loss would not reflect actual losses of wood or leaf mass, we did not allow any such value to decrease over time for an individual, instead retaining the previous survey's value. We then summarized all variables by survey and species and examined trends over time.

RESULTS

Allometric Equations

The best allometric equations for predicting whole-tree quantities included two variables, either *f*DBH and height or *f*DBH and crown volume. Goodness of fit was consistently high, with no R^2 values below 0.87 (Table 2). Equations using *f*DBH as the sole predictor performed more poorly, but all R^2 values still exceeded 0.79 (Table 1).

Table 1. Allometric equations for predicting total aboveground quantities of *Sequoia sempervirens* in second-growth forests using functional diameter at breast height (*f*DBH; units cm). The equation form for all models is $a(fDBH)^b$.

Dependent variable	*a*	*b*	*N*	R^2
Total mass (Mg)	1.78E-04	2.24E+00	34	0.925
Total volume (m^3)	5.08E-04	2.24E+00	34	0.924
Wood volume (m^3)	4.24E-04	2.22E+00	34	0.933
Heartwood volume (m^3)	7.49E-05	2.48E+00	34	0.910
Bark area (m^2)	6.50E-01	1.48E+00	34	0.859
Cambium area (m^2)	1.31E-01	1.68E+00	34	0.864
Heartwood area (m^2)	1.95E-02	1.77E+00	34	0.874
Leaf mass (kg)	7.34E-02	1.59E+00	34	0.815
Leaf area (m^2)	6.27E-01	1.52E+00	34	0.792
Millions of leaves	4.18E-02	1.58E+00	34	0.829

Table 2. Allometric equations for predicting total aboveground quantities of *Sequoia sempervirens* in second-growth forests using multiple ground-based measurements. The equation form for all models is $aV1^b + cV2^d$.

Dependent variable	V1	V2	*a*	*B*	*C*	*d*	*N*	R^2
Total mass (Mg)	*f*DBH (cm)	Height (m)	2.67E-04	2.14E+00	2.33E-32	1.71E+01	34	0.985
Total volume (m^3)	*f*DBH (cm)	Height (m)	7.34E-04	2.14E+00	1.11E-35	1.91E+01	34	0.984
Wood volume (m^3)	*f*DBH (cm)	Height (m)	6.21E-04	2.12E+00	1.01E-30	1.64E+01	34	0.982
Heartwood volume (m^3)	*f*DBH (cm)	Height (m)	1.04E-04	2.38E+00	3.97E-28	1.50E+01	34	0.985
Bark area (m^2)	*f*DBH (cm)	Crown volume (m^3)	6.26E-01	1.41E+00	5.68E-01	7.98E-01	34	0.902
Cambium area (m^2)	*f*DBH (cm)	Crown volume (m^3)	1.49E-01	1.57E+00	1.12E-01	9.35E-01	34	0.927
Heartwood area (m^2)	*f*DBH (cm)	Height (m)	4.16E-02	1.56E+00	2.47E-12	7.20E+00	34	0.954
Leaf mass (kg)	*f*DBH (cm)	Crown volume (m^3)	9.91E-02	1.44E+00	4.53E-02	9.31E-01	34	0.886
Leaf area (m^2)	*f*DBH (cm)	Crown volume (m^3)	8.43E-01	1.35E+00	4.59E-01	8.77E-01	34	0.873
Millions of leaves	*f*DBH (cm)	Crown volume (m^3)	6.76E-02	1.41E+00	9.80E-03	1.01E+00	34	0.882

Growth Reconstructions

We climbed and mapped four trees with a total of 298 live appendages (Table 3). Fifty-two ring series were obtained from increment cores with a total of 4344 annual rings, 94% of which were cross-dated with high confidence. Height, DBH, and main trunk volume were reconstructed backwards between 107 and 122 years, depending on the oldest annual ring obtained on each tree. Twelve surveyed height measurements from the four trees were an average of 2.2 m different from reconstructed values, all but one being less than the reconstructed value (Figure 1). For *Picea*, surveyed DBH measurements averaged 12.4 cm below reconstructed values, while *Sequoia* surveyed DBH measurements averaged only 2.8 cm different from reconstructed values (Figure 1). Trends in reconstructed trunk growth closely matched trends in trunk growth allometrically predicted from reconstructed DBH and height, although they frequently differed in magnitude (Figure 2). Values from allometric prediction were below the whole-trunk reconstruction in 63%, 75%, 39%, and 86% of years for, respectively, SESE1, SESE2, PISI1, and PISI2.

Table 3. Characteristics of two *Sequoia sempervirens* and two *Picea sitchensis* trees climbed and intensively measured in the Metcalf plots.

Tree	*f*DBH (cm)	DTB (cm)	Height (m)	Number of ring series	Earliest cross-dated year
SESE1	136.5	133.0	57.1	10	1884
SESE2	90.0	90.2	53.1	12	1882
PISI1	136.4	91.4	63.4	12	1897
PISI2	147.8	135.2	65.5	18	1891

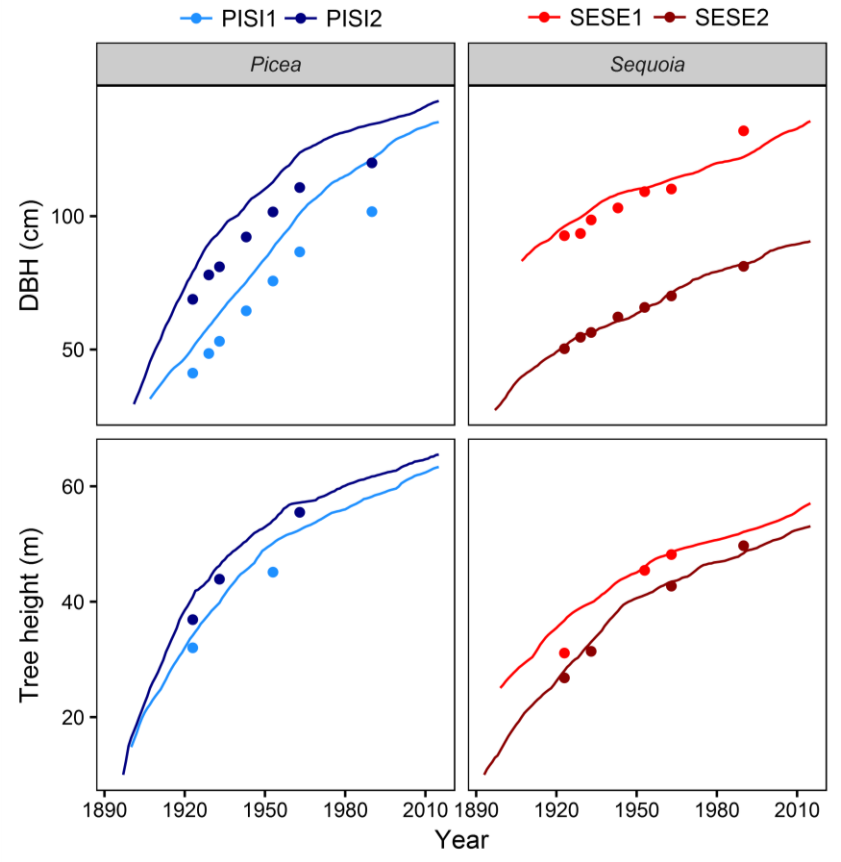

Figure 1. Reconstructed versus measured height and DBH for four trees in the Metcalf plots. Lines represent reconstructions based on annual ring widths, and dots represent historical survey measurements.

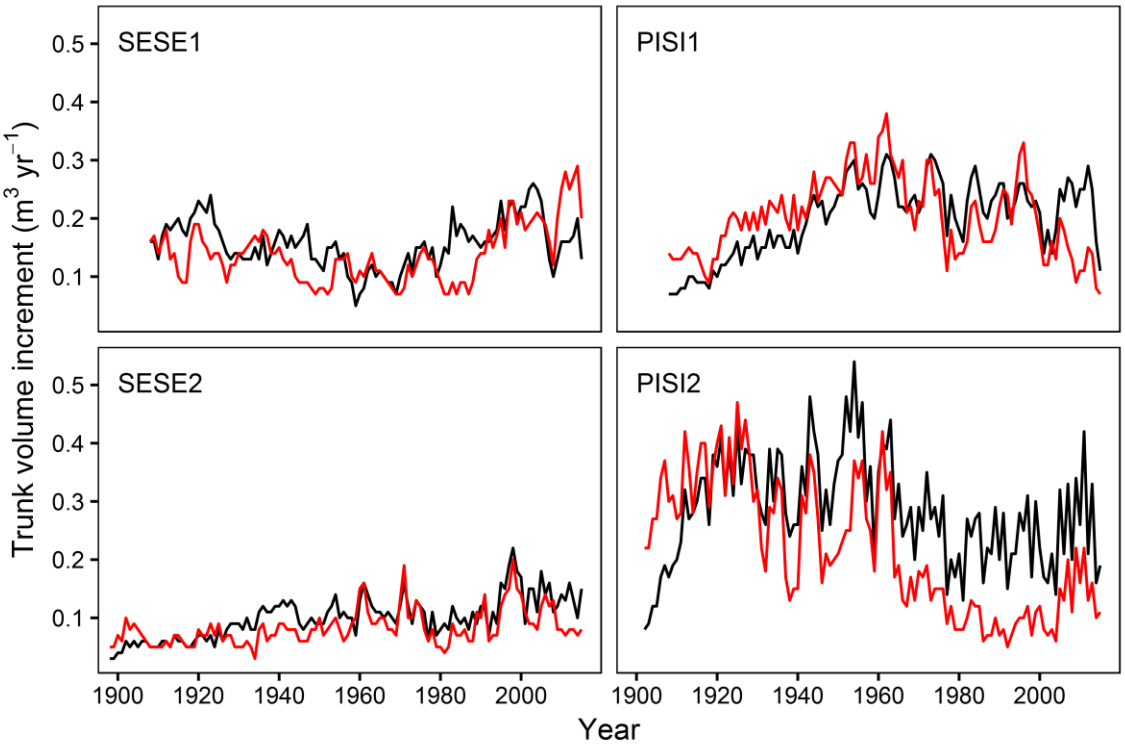

Figure 2. Whole-trunk reconstruction (black lines) versus allometric prediction (red lines) based on reconstructed DBH and tree height for trunk volume increments of four trees in the Metcalf plots.

Plot Surveys

We tagged and measured 114 trees in Plot 1 and 144 trees in Plot 2. Applying allometric equations to all tagged trees yielded detailed predictions of plot-level aboveground quantities (Table 4 and Table 5). *Sequoia* dominated all categories in both plots, although *Picea* in Plot 1 and *Abies* in Plot 2 were large contributors. Accordingly, Plot 2 totals artificially appeared low for quantities where *Abies* could not be included due to lack of an allometric equation.

Table 4. Plot-level totals for aboveground tree mass and volume quantities in the Metcalf plots. Allometric equations for *Abies* from published source did not allow for calculation of standard error. Dashes (—) indicate that an equation was not available for that species and quantity.

Plot	Year	Species	Total mass (Mg ha^{-1})	Total volume (m^3 ha^{-1})	*Abies* trunk volume (m^3 ha^{-1})	Wood volume (m^3 ha^{-1})	Sapwood volume (m^3 ha^{-1})	Heartwood volume (m^3 ha^{-1})	Bark volume (m^3 ha^{-1})
1	**2013**	*Abies*	13	—	30	—	—	—	—
		Picea	213 ± 24	480 ± 29	—	417 ± 27	91 ± 4	326 ± 23	62 ± 3
		Pseudotsuga	107 ± 24	258 ± 55	—	197 ± 49	36 ± 15	161 ± 34	61 ± 6
		Sequoia	586 ± 37	1612 ± 102	—	1246 ± 83	561 ± 32	685 ± 50	367 ± 20
		TOTAL	919 ± 85[a]	2349 ± 186[b]	30	1859 ± 159[b]	688 ± 51[b]	1172 ± 108[b]	489 ± 29[b]
2	**2015**	*Abies*	326	—	597	—	—	—	—
		Picea	97 ± 13	211 ± 13	—	184 ± 12	40 ± 2	144 ± 10	27 ± 1
		Pseudotsuga	41 ± 7	101 ± 16	—	78 ± 14	15 ± 4	63 ± 10	23 ± 2
		Sequoia	621 ± 46	1709 ± 130	—	1325 ± 105	628 ± 43	697 ± 62	388 ± 25
		TOTAL	1086 ± 67[a]	2022 ± 158[b]	597	1586 ± 131[b]	683 ± 48[b]	904 ± 82[b]	438 ± 29[b]

a: *Abies* component was included in total but not in error term.
b: Total does not include *Abies* component.

Table 5. Plot-level totals for aboveground tree live tissue and leaf quantities in the Metcalf plots. Allometric equations for *Abies* from published source did not allow for calculation of standard error. Dashes (—) indicate that an equation was not available for that species and quantity.

Plot	Year	Species	Bark area (m^2 ha^{-1})	Cambium area (m^2 ha^{-1})	Heartwood area (m^2 ha^{-1})	Leaf mass (kg ha^{-1})	Leaf area (m^2 ha^{-1})	Millions of leaves ha^{-1}
1	**2013**	*Abies*	—	—	—	187	439	—
		Picea	20075 ± 1812	13236 ± 1154	2555 ± 182	4702 ± 469	21136 ± 2313	1092 ± 126
		Pseudotsuga	2660 ± 803	1805 ± 312	1343 ± 244	671 ± 128	3530 ± 699	269 ± 47
		Sequoia	64387 ± 10221	31261 ± 4965	7062 ± 728	11906 ± 2340	72091 ± 14712	6512 ± 1205
		TOTAL	87122 ± 12836[b]	46302 ± 6431[b]	10960 ± 1153[b]	17464 ± 2937[a]	96758 ± 17723[a]	7872 ± 1379[b]
2	**2015**	*Abies*	—	—	—	4236	9737	—
		Picea	9051 ± 844	5953 ± 527	1159 ± 102	2125 ± 217	9547 ± 1075	493 ± 59
		Pseudotsuga	1021 ± 301	683 ± 107	500 ± 76	245 ± 43	1297 ± 231	97 ± 16
		Sequoia	80845 ± 12208	38416 ± 5964	7997 ± 964	14867 ± 2850	91649 ± 17932	8031 ± 1489
		TOTAL	90917 ± 13353[b]	45052 ± 6598[b]	9657 ± 1141[b]	21473 ± 3110[a]	102493 ± 19239[a]	8621 ± 1564[b]

a: *Abies* component was included in total but not in error term.
b: Total does not include *Abies* component.

Despite having only hand-drawn maps from 1990, linking trees among the Metcalf surveys, the Becking 1990 survey, and the current survey was largely successful. For current trees assumed not to be ingrowth based on size (> 40 cm DBH), only three between both plots could not be linked to historical measurements. All trees from the 1990 survey were accounted for in the present. However, six now-dead trees from 1990 could not be linked to pre-1990 IDs and were too large to be ingrowth. Thirteen trees were missed in individual surveys, seven of which were in 1990, and their DBH values were interpolated based on prior and subsequent measurements.

We examined trends over time once all possible trees were identified and linked across surveys. Mean and maximum DBH both increased and stem density decreased, while maximum height was inconsistent due to the haphazard subset of trees measured (Table 6). Basal area approximately doubled in both plots, reaching 124 and 143 m^2 ha^{-1} in Plots 1 and 2, respectively. *Sequoia* represented an increasing proportion of basal area (Figure 3). Non-*Sequoia* species decreased in number while slowly increasing in basal area, excepting the near-loss of *Abies* basal area in Plot 1. Small numbers of *Alnus* and *Tsuga* were initially present in Plots 1 and 2, respectively, but they dropped out by 1953.

Mortality rates were variable in both plots and ranged from 0.3 to 2.7% trees yr^{-1} (Table 7). In Plot 1, recruitment was absent in the first half of the study period and then climbed above mortality. In Plot 2, early recruitment could plausibly have been trees missed in the first survey, but records did not indicate either way. Recruitment rates increased in the second half of the study period for Plot 2 but not above mortality rates as in Plot 1.

Table 6. Summary statistics for the Metcalf plots, 1923-2015. Maximum height is only within the subset of trees measured for height in each survey. Dashes (—) indicate years in which no heights were measured.

Plot	Year	Trees per hectare	Mean DBH (cm)	Max DBH (cm)	Max height (m)	*Sequoia* mean DBH (cm)	*Sequoia* max height (m)
1	1923	435	39.3	109.0	43.0	38.5	33.5
	1929	423	42.2	111.8	—	40.9	—
	1933	378	45.7	112.0	48.8	42.7	44.8
	1943	353	50.8	114.0	—	47.1	—
	1953	309	55.9	116.6	57.9	51.2	55.5
	1963	272	60.2	117.9	56.7	54.1	51.8
	1990	274	60.3	137.5	53.3	55.3	53.3
	2013	282	62.2	157.8	65.1	57.8	59.8
2	1923	596	32.9	85.1	41.1	30.5	37.5
	1929	593	35.3	90.9	—	32.6	—
	1933	578	36.7	91.9	43.9	33.8	40.2
	1943	534	41.6	101.1	44.2	37.7	44.2
	1953	482	45.8	107.7	48.8	41.4	48.8
	1963	398	51.6	113.8	55.5	46.2	48.2
	1990	368	58.8	127.7	57.0	52.1	49.7
	2015	356	62.8	146.5	65.3	56.9	57.0

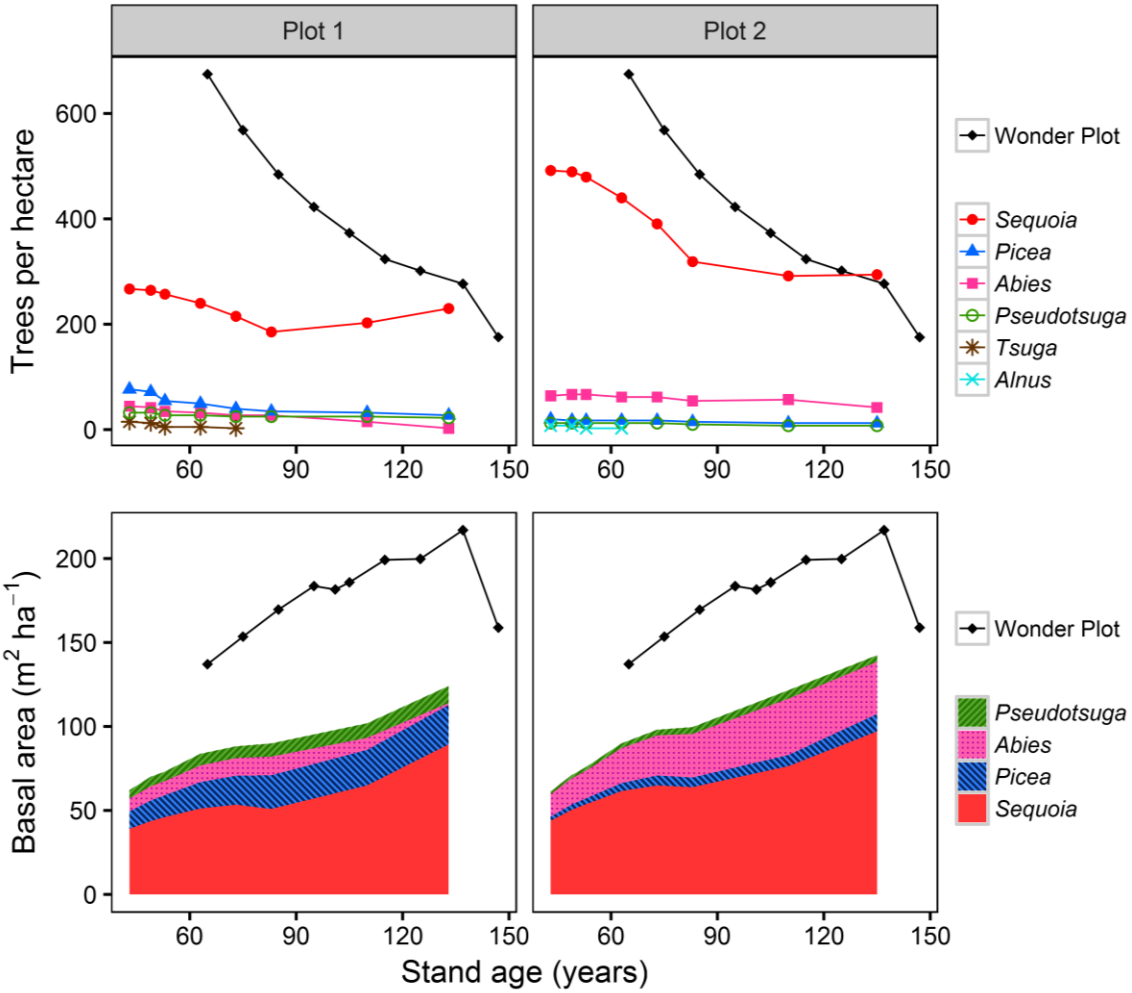

Figure 3. Basal area and stem density over time in the Metcalf plots. Fritz Wonder Plot, in a pure *Sequoia* stand, is presented for comparison (data from Gerhart, 2006).

Table 7. Recruitment and mortality rates in the Metcalf plots.

Plot	Interval	Recruitment (no. of trees)	Mortality (no. of trees)	Recruitment (trees ha^{-1} yr^{-1})	Mortality (trees ha^{-1} yr^{-1})	Mortality (% yr^{-1})
1	1923-1929	0	5	0.0	2.1	0.5%
	1929-1933	0	18	0.0	11.1	2.7%
	1933-1943	0	10	0.0	2.5	0.7%
	1943-1953	0	18	0.0	4.4	1.3%
	1953-1963	0	15	0.0	3.7	1.3%
	1963-1990	18	17	1.6	1.6	0.6%
	1990-2013	19	16	2.0	1.7	0.7%
2	1923-1929	4	5	1.6	2.1	0.3%
	1929-1933	2	8	1.2	4.9	0.8%
	1933-1943	1	19	0.2	4.7	0.8%
	1943-1953	0	21	0.0	5.2	1.0%
	1953-1963	2	36	0.5	8.9	2.0%
	1963-1990	6	25	0.5	2.3	0.6%
	1990-2015	10	21	1.0	2.1	0.6%

Diameter distributions of each species change considerably over time (Figure 4 and Figure 5). The non-*Sequoia* cohorts shifted upwards in range with very few trees recruited into the smaller size classes. *Sequoia* in both plots began with a right-skewed distribution, especially evident in Plot 2, but gradually shifted to a broader, more uniform distribution.

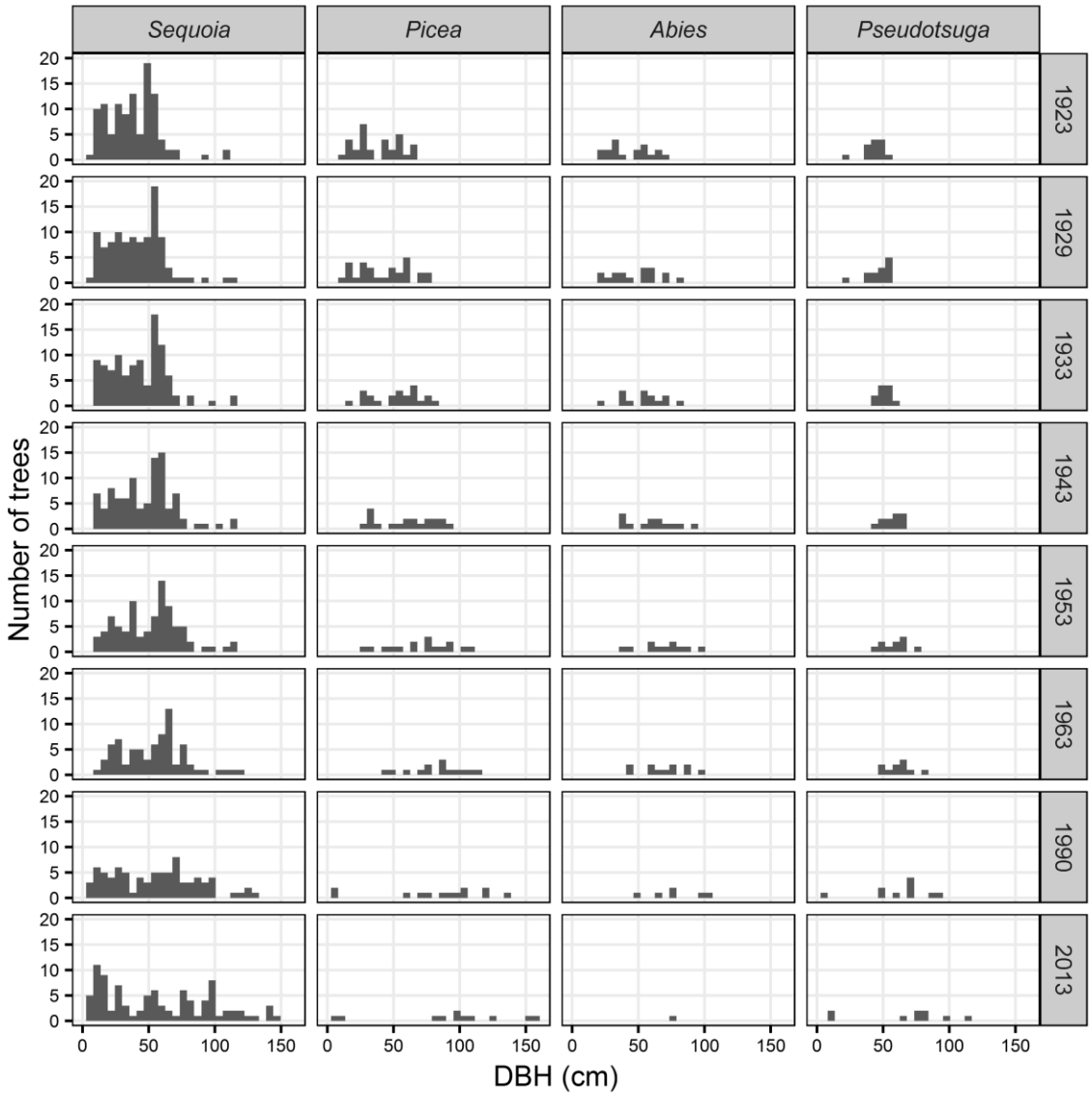

Figure 4. Diameter distributions over time of the major tree species in Plot 1.

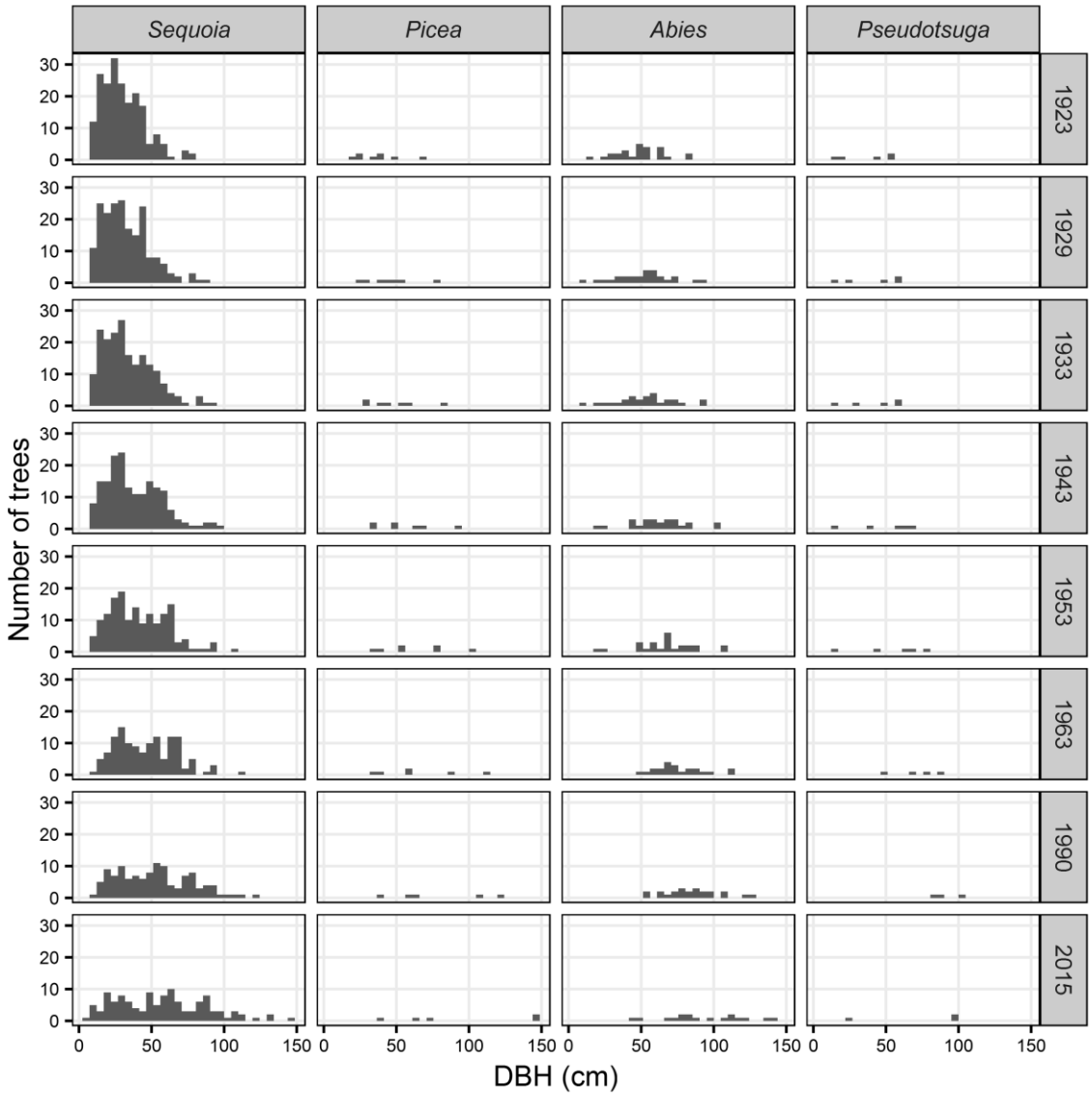

Figure 5. Diameter distributions over time of the major tree species in Plot 2.

DISCUSSION

We completed the most detailed survey of a second-growth *Sequoia* forest to date, using new allometric equations combined with measurements obtained from the ground, tree climbing, and LiDAR. We also intensively measured four trees via crown mapping and dendrochronology, allowing us to check survey methodology against annually resolved tree-ring measurements. With repeated surveys reaching back to 1923, the Metcalf plots offer a rare view of *Sequoia* forest development after logging.

Growth Reconstructions

Dendrochronological reconstructions of radial and apical growth in *Picea* and *Sequoia* found that measurements taken from 1923 to 1990 could largely be trusted (Figure 1). The height measurements, likely taken with clinometers, were remarkably close to reconstructed values, considering the difficulty of measuring trees in tall forests. The small errors present are biased towards underestimation of height. Diameter measurements for *Sequoia* were also accurate, although an obvious discrepancy in 1990 for SESE1 is likely a demonstration of human error. In *Picea,* diameter is systematically lower for survey measurements as compared to the reconstruction. Most likely, the cause is the diameter tape being wrapped around the trunk above breast height, avoiding *Picea*'s large buttresses, either by choice or through a different method of assessing ground level. However, if previous surveys assessed ground level differently for all trees, diameter measurements for *Sequoia* should have also been lower than reconstructions. It

also seems unlikely that the reconstruction is instead overestimating diameter, as this would imply systematic underestimates of radial growth. Consistent underestimation of annual growth would result in a trend of increasing differences between the reconstruction and survey measurements as time moves backwards, and the opposite is true (Figure 1). This discrepancy for *Picea* indicates that plot-level quantities for *Picea* calculated from the historical surveys may be overestimates. For *Sequoia*, however, two trees confirm the reliability of repeated measurements since 1923 for tracking diameter and height growth.

We also compared reconstructed main trunk wood volume increments to those computed by applying allometric equations to reconstructed trunk diameters and heights. Despite differences in growth increments, trends resulting from the two methods closely mirrored each other in all four trees (Figure 2). Differences in magnitude probably reflect disconnects between radial increments at ground level and along the entire trunk (Ishii et al., 2017). Larger discrepancies for *Picea* may be connected to the inconsistency of reconstructing functional diameter with ring widths on trees with strong buttressing. The allometric reconstruction was usually lower for three of the four trees, indicating larger radial increments in the upper section of the trunk in those time periods. While accessing the entire tree to reconstruct trunk wood growth revealed dynamics invisible from the ground, allometric equations yielded reasonably accurate growth estimates.

Growth and Demography

Trends over time in the plots reflected deterministic processes of stand development as well as the stochastic influence of disturbances and mortality (Franklin et al., 2002). Biomass rapidly accumulated over the study period, and mean tree size increased as stem density decreased (Table 6). Non-*Sequoia* slowly dropped in number as they succumbed to basal decay and windthrow (Figure 3), although the surviving trees were steadily growing dominants (Figure 4 and Figure 5). The large *Abies* remaining in Plot 2 were heavily leaning and appeared likely to die in the near future. With the decline of other species, *Sequoia* dominance increased in the plots, especially starting around 80 years post-logging (Figure 3).

Plot mortality rates were variable, reflecting the stochastic processes that drive tree mortality (Franklin et al., 1987). Although individual causes of tree death were rarely recorded, survey notes described large windthrow events between 1943 and 1963, and they had a clear impact on mortality in both plots (Table 7). Net growth was also impacted, as seen by the plateau in total basal area during that period (Figure 3). In the second half of the study period, an understory of trees was beginning to establish (Table 7). In Plot 1, recruitment even rose slightly above mortality in the last time interval. Correspondingly, the *Sequoia* populations in both plots increased their size range, as canopy dominants grew and recruitment filled in the smallest size classes (Figure 4 and Figure 5). The size distributions of *Sequoia* also flattened over time, moving from a high proportion of small trees to a heterogeneous mix of tree sizes, similar to distributions found in old-growth *Sequoia* forest (Russell and Michels, 2011).

There were no clear and interpretable influences on growth or demography trends in the thinned halves of either plot. A small proportion of basal area was removed (~18%) in both the low thin in Plot 1 and the non-*Sequoia* crown thin in Plot 2, likely not enough to observe differences from a control, especially considering the small area treated (0.2 ha). Even the lightest treatments in most thinning studies remove at least 25% of basal area (Chittick et al., 2007; Oliver et al., 1994; Plummer et al., 2012). Metcalf began planning in the 1950s to open up more growing space with another thinning treatment, but the plan never materialized.

Comparisons

The only similar long-term permanent observation plot for second-growth *Sequoia* forest is Emanuel Fritz's Wonder Plot in Mendocino County, famous for its high rate of tree growth (Allen et al., 1996; Fritz, 1945; Gerhart, 2006). Established by a collaborator of Metcalf, also in 1923, this pure *Sequoia* alluvial forest provided an interesting comparison with the mixed-species Metcalf plots farther north in the *Sequoia* range. Stem density in the Wonder Plot was higher than the Metcalf plots around 60 years post-logging but declined steeply to similar levels by 130 years (Figure 3). Tree growth in the Wonder Plot outpaced the Metcalf plots by a large margin with approximately one-and-a-half times the basal area at equivalent ages. However, a 1998 windthrow event in the Wonder Plot all but erased that margin. The most recent Wonder Plot survey found a total basal area that will be nearly equivalent to the Metcalf plots if growth trends continue (Figure 3). Considering that Fritz intentionally placed his plot in "the best of the

second-growth on Big River" (Fritz, 1945), it is unsurprising that tree growth in the Metcalf plots did not approach the rates of the Wonder Plot.

The other comparable example of research on unmanaged second-growth *Sequoia* forests was a chronosequence study, also in Mendocino County (Russell and Michels, 2011). The chronosequence spanned zero to 130 years of forest ages and average basal area was similar to the Metcalf plots at equivalent ages, although the Metcalf plots surpassed the chronosequence at the endpoint (124 and 142 m^2 ha^{-1} for Metcalf versus 103 m^2 ha^{-1} for the chronosequence). They also observed similar trends in the increasing dominance of *Sequoia*, despite a different mix of tree species.

Our application of allometric models predicting total mass and leaf area also permitted comparison to old-growth *Sequoia* forests described in detail in Van Pelt et al. (2016). We selected four plots from Van Pelt et al. (2016) for comparison, two in Redwood National Park and two in Prairie Creek Redwoods State Park, which were the closest geographically and ecologically to the Metcalf plots. At approximately 135 years since logging, both Metcalf plots were near the bottom end of the range for their old-growth counterparts in leaf area index of trees alone. Unsurprisingly, the Metcalf plots lagged far behind the old-growth forests in total aboveground tree mass with the old-growth plots being between three and four times heavier (Figure 6). These results provide further support for maximum tree LAI for *Sequoia* forests being approximately 15, regardless of forest age (Berrill and O'Hara, 2007; Van Pelt et al., 2016). Plot 2 is near to that theoretical maximum, while Plot 1 falls below, probably due to recent losses of large non-*Sequoia*. While the second-growth forest in the Metcalf plots had similar

photosynthetic capacity after 135 years of growth, trees in old-growth forests had been utilizing that capacity for many centuries and storing the energy in decay-resistant heartwood. Total LAI was still greater in old-growth forests due to their understory component (Van Pelt et al., 2016), which the Metcalf plots have only just begun to develop.

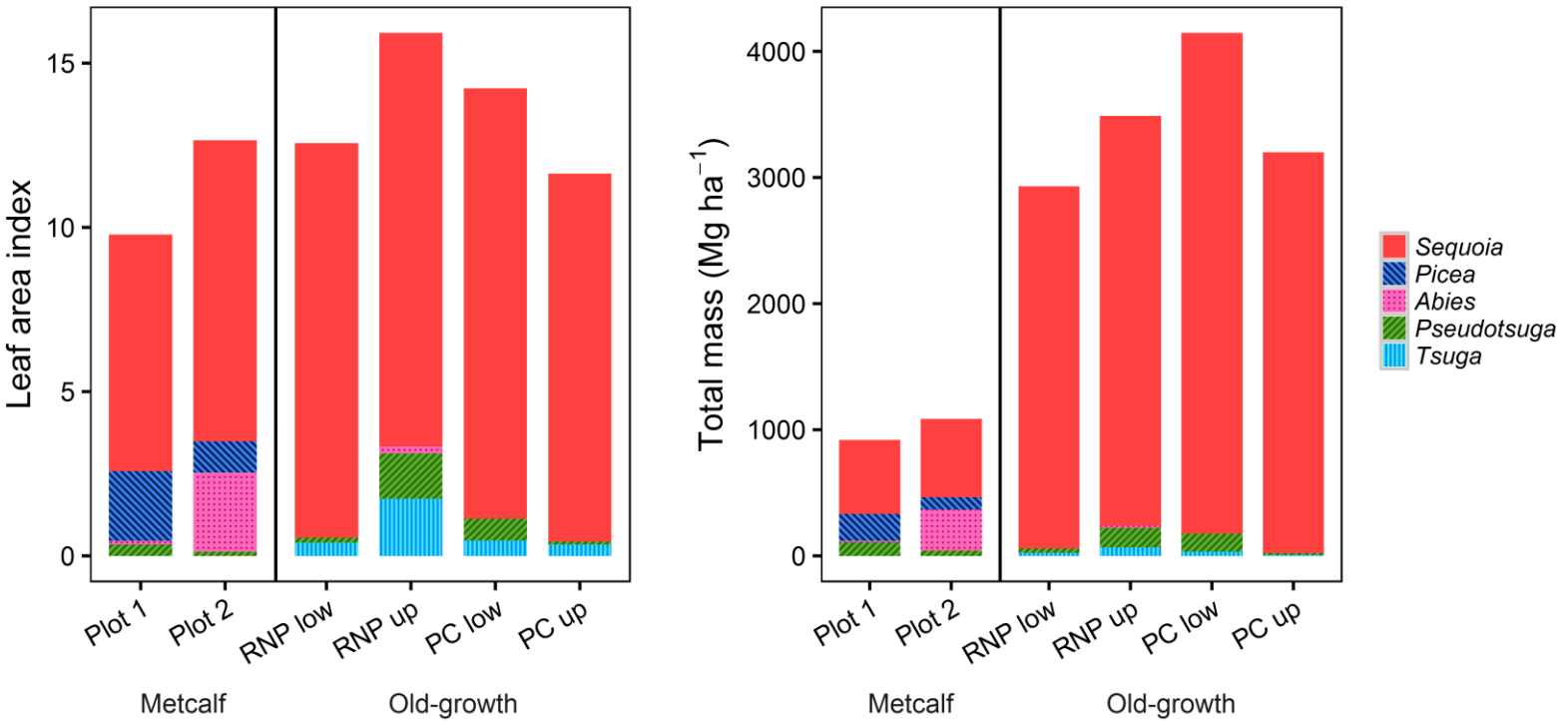

Figure 6. Total tree mass and leaf area index of the Metcalf plots at ~135 years post-logging compared with two lowland and two upland plots in old-growth forest from Van Pelt et al. (2016) in Redwood National Park (RNP) and Prairie Creek Redwoods State Park (PC).

Conclusions and Further Study

The Metcalf plots demonstrated sustained growth over the study period, although not approaching the rates achieved by Fritz's Wonder Plot (Gerhart, 2006). Steady growth occurred despite heavy human use within and around the plots, even predating the establishment of the city park in 1955, according to survey notes. Undergrowth was clearly reduced by formal and social trails in the plots, particularly in the upper plot, and soil compaction was likely. The lack of notable impact from recreational use on tree populations points towards the potential for balance between ecological and social objectives in forest restoration planning.

The non-*Sequoia* component in the plots exhibited rapid growth, but the trees are slowly dying and likely to be replaced by shade-tolerant *Sequoia*. This process and the accompanying increase in the dominance of *Sequoia* likely marks the transition out of the biomass accumulation stage and into the maturation stage of forest development after a stand-replacing disturbance (Franklin et al., 2002). The 1963 survey (~83 years post-logging) could be pinpointed as the transition boundary, although mortality in the two previous decades is dominated by density-independent factors (windstorms), also characteristic of the maturation stage. Earlier transitions, such as canopy closure, occurred before the plots were established. As the forest progresses through the maturation stage, we expect continued growth and dominance by *Sequoia*, understory development of trees and shrubs, and accumulation of individual tree structure through damage and reiteration (Sillett and Van Pelt, 2007).

Restoration of old-growth forest attributes in second-growth *Sequoia* forests through silvicultural manipulation is of increasing interest. Our results from relatively unmanaged conditions can be compared to such studies, especially as treated stands move beyond rotation age. The large non-*Sequoia* component occupying growing space in the Metcalf plots, as well as the exceptional example of growth in the Wonder Plot, indicate opportunities for acceleration of second-growth forests toward the old-growth condition. Recent results also suggest that more than one thinning treatment is necessary for marked increases in tree growth (Berrill et al., 2013), which supports the lack of effect from thinning here.

New research efforts in mature second-growth *Sequoia* forests could be valuable beyond simply increasing the small number of studies. In future surveys of the Metcalf plots, or in other locations, the inclusion of woody debris and non-tree vegetation would be particularly interesting, allowing for complete biomass and carbon accounting. Highly productive patches of forest throughout the *Sequoia* range could be targeted to discover if Fritz's Wonder Plot represents the upper limit of growth rate. Permanent plots in the drier southern end of the *Sequoia* range would be novel, and possibly critical considering an impending drier and more extreme climate. Regardless of a change in scope, with further observation and protection from human disturbances the Metcalf plots could continue to provide a valuable point of comparison as they naturally develop into an old-growth *Sequoia* forest.

LITERATURE CITED

Allen, G., Lindquist, J., Melo, J., Stuart, J., 1996. Seventy-two years' growth on a redwood sample plot: the wonder plot revisited, in: Proceedings of the Conference on Coast Redwood Forest Ecology and Management. pp. 61–62.

Berrill, J.-P., Beal, C.B., LaFever, D.H., Dagley, C.M., 2013. Modeling Young Stand Development towards the Old-Growth Reference Condition in Evergreen Mixed-Conifer Stands at Headwaters Forest Reserve, California. Forests 4, 455–470. doi:10.3390/f4020455

Berrill, J.-P., O'Hara, K.L., 2007. Patterns of leaf area and growing space efficiency in young even-aged and multiaged coast redwood stands. Canadian Journal of Forest Research 37, 617–626.

Busing, R.T., Fujimori, T., 2002. Dynamics of composition and structure in an old *Sequoia sempervirens* forest. Journal of Vegetation Science 13, 785–792.

Carroll, A.L., Sillett, S.C., Kramer, R.D., 2014. Millennium-Scale Crossdating and Inter-Annual Climate Sensitivities of Standing California Redwoods. PLoS ONE 9, e102545. doi:10.1371/journal.pone.0102545

Chittick, A.J., Keyes, C.R., others, 2007. Holter Ridge thinning study, Redwood National Park: preliminary results of a 25-year retrospective, in: Proceedings of the Redwood Region Forest Science Symposium: What Does the Future Hold. USDA Forest Service General Technical Report PSW-GTR-194, pp. 271–280.

Coonen, E.J., Sillett, S.C., 2015. Separating effects of crown structure and competition for light on trunk growth of *Sequoia sempervirens*. Forest Ecology and Management 358, 26–40. doi:10.1016/j.foreco.2015.08.035

Del Tredici, P., 1998. Lignotubers in *Sequoia sempervirens*: development and ecological significance. Madroño 45, 255–260.

Franklin, J.F., Shugart, H.H., Harmon, M.E., 1987. Tree death as an ecological process. BioScience 37, 550–556. doi:10.2307/1310665

Franklin, J.F., Spies, T.A., Pelt, R.V., Carey, A.B., Thornburgh, D.A., Berg, D.R., Lindenmayer, D.B., Harmon, M.E., Keeton, W.S., Shaw, D.C., 2002. Disturbances and structural development of natural forest ecosystems with silvicultural implications, using Douglas-fir forests as an example. Forest Ecology and Management 155, 399–423.

Fritz, E., 1945. Twenty Years' Growth on a Redwood Sample Plot. Journal of Forestry 43, 30–36.

Gerhart, M., 2006. Expanding the legacy of research at the Fritz Wonder Plot, Big River, California: A report to Save-the-Redwoods League. Mendocino Land Trust, Mendocino, CA.

Holmes, R.L., 1983. Computer-assisted quality control in tree-ring dating and measurement. Tree-ring bulletin 43, 69–78.

Ishii, H.R., Sillett, S.C., Carroll, A.L., 2017. Crown dynamics and wood production of Douglas-fir trees in an old-growth forest. Forest Ecology and Management 384, 157–168.

Lindquist, J.L., 2004. Growth and yield report for the Whiskey Springs redwood commercial thinning study. California Forestry Report.

Lorimer, C.G., Porter, D.J., Madej, M.A., Stuart, J.D., Veirs Jr., S.D., Norman, S.P., O'Hara, K.L., Libby, W.J., 2009. Presettlement and modern disturbance regimes in coast redwood forests: Implications for the conservation of old-growth stands. Forest Ecology and Management 258, 1038–1054. doi:10.1016/j.foreco.2009.07.008

Neal, R.L., 1967. Sprouting of old-growth redwood stumps, first year after logging (USDA Forest Service Research Note PSW-137). Southwest Forest and Range Experiment Station, Berkeley, CA.

Noss, R.F. (Ed.), 2000. The redwood forest: history, ecology, and conservation of the coast redwoods. Island Press, Washington DC.

Oliver, W.W., Lindquist, J.L., Strothmann, R.O., 1994. Young-growth redwood stands respond well to various thinning intensities. Western Journal of Applied Forestry 9, 106–112.

Plummer, J.F., Keyes, C.R., Varner, J.M., 2012. Early-Stage thinning for the restoration of young redwood—Douglas-fir forests in northern coastal California, USA. International Scholarly Research Notices 2012.

QGIS Development Team, 2012. QGIS Geographic Information System. Open Source Geospatial Foundation Project.

Russell, W., Michels, K.H., 2011. Stand development on a 127-yr chronosequence of naturally regenerating *Sequoia sempervirens* (Taxodiaceae) forests. Madrono 57, 229–241.

Sawyer, J.O., Gray, J., West, G.J., Thornburgh, D.A., Noss, R.F., Engbeck Jr, J.H., Marcot, B.G., Raymond, R., 2000. History of redwood and redwood forests, in: Noss, R.F. (Ed.), The Redwood Forest: History, Ecology, and Conservation of the Coast Redwoods. Island Press, Washington DC, pp. 7–38.

Sawyer, J.O., Sillett, S.C., Popenoe, J.H., LaBanca, A., Sholars, T., Largent, D.L., Euphrat, F., Noss, R.F., Van Pelt, R., 2000. Characteristics of redwood forests, in: Noss, R.F. (Ed.), The Redwood Forest: History, Ecology, and Conservation of the Coast Redwoods. Island Press, Washington DC, pp. 39–80.

Sillett, S.C., Van Pelt, R., 2007. Trunk reiteration promotes epiphytes and water storage in an old-growth redwood forest canopy. Ecological Monographs 77, 335–359.

Sillett, S.C., Van Pelt, R., Carroll, A.L., Kramer, R.D., Ambrose, A.R., Trask, D., 2015. How do tree structure and old age affect growth potential of California redwoods? Ecological Monographs 85, 181–212. doi:10.1890/14-1016.1

Standish, J.T., Manning, G.H., Demaerschalk, J.P., 1985. Development of biomass equations for British Columbia tree species 264.

Teraoka, J.R., 2012. Forest Restoration at Redwood National Park: a Case Study of an Emerging Program, in: Proceedings of the Coast Redwood Forests in a Changing

California: A Symposium for Scientists and Managers. General Technical Report PSW-GTR-238. US Department of Agriculture, Forest Service, Pacific Southwest Research Station, pp. 561–569.

Thornburgh, D.A., Noss, R.F., Angelides, D.P., Olson, C.M., Euphrat, F., Welsh, H.H.J., 2000. Managing redwoods, in: Noss, R.F. (Ed.), The Redwood Forest: History, Ecology, and Conservation of the Coast Redwoods. Island Press, Washington DC, pp. 229–261.

Van Kirk, S., 1985. A History of the Arcata Community Forest. Unpublished research paper, Arcata, CA: Humboldt County Library.

Van Pelt, R., Sillett, S.C., Kruse, W.A., Freund, J.A., Kramer, R.D., 2016. Emergent crowns and light-use complementarity lead to global maximum biomass and leaf area in *Sequoia sempervirens* forests. Forest Ecology and Management 375, 279–308. doi:10.1016/j.foreco.2016.05.018

Webb, L.A., Lindquist, J.L., Wahl, E., Hubbs, A., 2012. Whiskey springs long-term coast redwood density management; final growth, sprout, and yield results, in: Proceedings of Coast Redwood Forests in a Changing California: A Symposium for Scientists and Managers. pp. 571–581.

Yamaguchi, D.K., 1991. A simple method for cross-dating increment cores from living trees. Canadian Journal of Forest Research 21, 414–416.